

ESTIMATING METHOD OF THE VARIATION IN EFFECTIVE PERMEABILITY OF HYDRATE-BEARING SANDS DURING HYDRATE DISSOCIATION BY DEPRESSURIZATION

Yanghui Li¹, Zhaoran Wu¹, Xiang Sun^{1*}, Yu Liu¹, Yongchen Song¹

1 Key Laboratory of Ocean Energy Utilization and Energy Conservation of Ministry of Education, Dalian University of Technology, Dalian 116024, China)

* corresponding author

ABSTRACT

Methane hydrate, a form of clean energy also called flammable ice, has drawn global interest as an alternative energy resource of traditional fossil energy. The rate of gas production using depressurization depends on the effective permeability of the formations, which is controlled by not only hydrate saturation but also the porosity change of the host sediment. A decrease in pore pressure leads to an increase in the effective stress and the collapse of the bonded structure made by the hydrate resulting in the volume contraction and permeability reduction. On the other hand, the pore pressure drop induces hydrate dissociation, which increases the volume of the pore and permeability. In this study, we conducted a series of experiments to measure the effective permeability of HBSs with different hydrate saturation. The relationship between porosity, hydrate saturation and effective permeability is analyzed. Combining the consolidation analysis, we proposed a new method to estimate the change in effective permeability of hydrate-bearing sands during dissociation by depressurization.

Keywords: permeability; soil compaction; hydrate dissociation; effective stress

1. INTRODUCTION

Clathrates of natural gas hydrates contain enormous energy reserves [1-2] and potential environment amity [3-5]. Depressurization, which reduces the pore fluid pressure from a wellbore and dissociates hydrate to gas, is a promising low-cost and highly efficient method to extract methane gas from the natural gas hydrate-

bearing sediments (HBSs) [6]. Permeability is a key factor to efficient gas production by depressurization as it affects both the motion of fluid and the temperature of the sediment, which are necessary conditions for hydrate dissociation [7-8].

At present, the permeability characteristics of hydrate-bearing reservoirs have been studied in many aspects by relevant researchers[9–14]. Although many researchers investigated the effects of hydrate existence on the permeability of HBSs, few published paper discussed the effect of compaction due to depressurization on the permeability.

In this paper, we extend the previous work about the effective permeability to analyze the effect of the soil compaction on the permeability of the HBSs. The relationship between the permeability and porosity and the relationship between the porosity and preconsolidation pressure are combined to estimate the variation in permeability of HBSs during hydrate dissociation by depressurization.

2. EXPERIMENT

2.1 Experimental apparatus

Fig.1 shows the experimental system adopted in this study. The system consists of an ISCO pump used for pore pressure control, an axial compression pump used for compacting soils, a Glycol water bath used for temperature control, a reaction chamber used for containing specimen, a differential pressure transducer used for measuring pressure loss, a back pressure valve and several devices for data transmission and signal processing. The temperature ranges from -243K to 363K

with a controlling precision is 0.05~0.1 K, which were controlled by the water bath (model XT5704LT-R30). The pore pressure of the hydrate-bearing sediments is supplied and controlled by an ISCO 260D pump. The differential pressure between the inlet and outlet of the reaction chamber is measured by a differential pressure sensor (ranges from 0 to 1MPa, with an accuracy of $\pm 0.01\text{kPa}$)

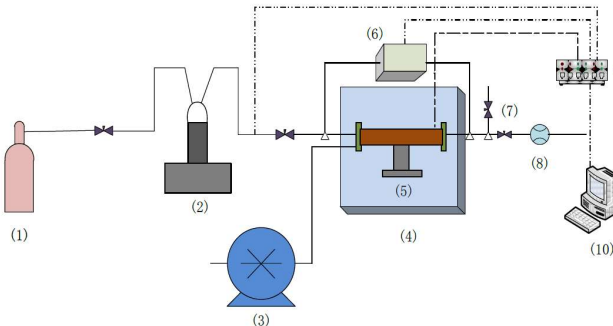


Fig. 1 scheme of the experimental system consisting of (1) CH₄ gas, (2) ISCO pump, (3) axial compression pump, (4) Glycol water bath, (5) reaction chamber, (6) differential pressure transducer, (7) exhaust, (8) back pressure valve, (9) A/D Module, (10)

2.2 Experimental procedure

The experimental procedure is similar to our previous work[12]. The difference is that in this study, the quartz sands are used as host sediments for forming the HBSs. The initial porosity is 42.7%. Initial pore pressure is set to 6MPa and temperature is kept at 274.15 K. The external load is exerted to make the specimen deforming. Table 1 shows the conditions of the experiment. Tests of No. 1-6 were done for the relationship between porosity and intrinsic permeability. Tests of No.7-9 were done for the relationship between hydrate saturation and effective permeability.

Table 1 The experimental conditions

No.	1	2	3	4	5	6	7	8	9
Hydrate saturation	0	0	0	0	0	0	0.1	0.25	0.45
External load(MPa)	0.1	1	3	5	7	9	6	6	6
Pore pressure at outlet(MPa)	0.1	0.1	0.1	0.1	0.1	0.1	6	6	6

2.3 Results and discussion

Fig.2 shows that the porosity decreases with the increasing effective stress, which means the compaction

makes HBSs dense and low compressible. The volume of pores decreases with the compaction influencing the permeability. As shown in Fig.3, the intrinsic permeability is positively proportional to porosity. Therefore, with the decrease in porosity due to compaction, intrinsic permeability decreases. The effective permeability decreases with hydrate saturation as shown in Fig.4. Hydrate occurrence habits change with hydrate saturation further affecting the relationship between hydrate saturation and effective permeability of HBSs[13].

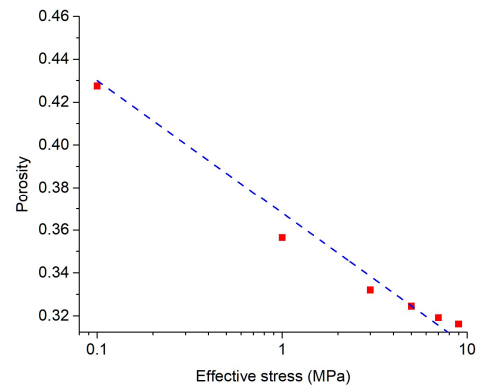


Fig.2 The effects of soil compaction on the porosity

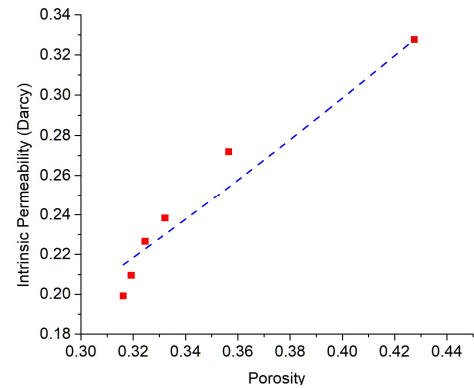


Fig.3 The relationship between porosity and intrinsic permeability

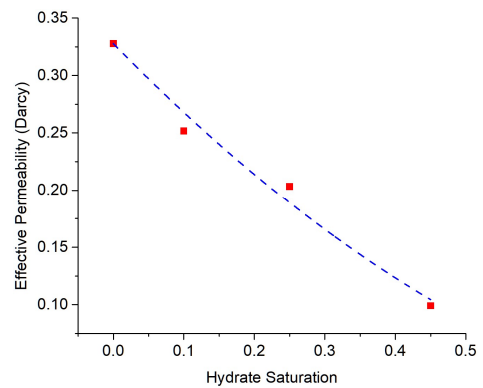


Fig.4 The relationship between hydrate saturation and effective permeability

3. ESTIMATING METHOD OF THE EFFECTIVE PERMEABILITY

Ren et al.[15] used the following expression to describe the relationship between porosity and intrinsic permeability.

$$K_{int} = K_{int0} \left(\frac{\phi}{\phi_0} \right)^\beta \quad (1)$$

where β is the model coefficient, K_{int0} is the initial intrinsic permeability, ϕ is porosity and ϕ_0 is initial porosity.

Masuda et al. [16] proposed a formula to describe the relationship between hydrate saturation and effective permeability.

$$K_{eff} = K_{int}(1 - s_h)^N \quad (2)$$

Therefore, combining (1) and (2), we have the permeability model describing the relationship among porosity, hydrate saturation and permeability.

According to the theory of soil mechanics, the compaction results in the decrease in porosity of the soil. For HBSs, the existence of hydrate has effects on the relationship between porosity and effective stress. Therefore, the compressibility of HBSs changes with hydrate dissociation.

$$\sigma' = \sigma'_0 \exp \left(\frac{\phi_0 - \phi}{\lambda_0 - a s_h^b} \right) \quad (3)$$

Here, σ' is the effective stress, λ_0 is the coefficient of compressibility of the host sediments. a and b are coefficients, which are related to hydrate saturation. σ'_0 is initial stress. We can get the relationship between effective stress and effective permeability.

$$K_{eff} = K_{int0} \left(1 - \frac{(\ln \sigma' - \ln \sigma'_0)(\lambda_0 - a s_h^b)}{\phi_0} \right)^\beta (1 - s_h)^N \quad (4)$$

According to the principle of effective stress, the decrease in pore pressure results in an increase in the effective stress as shown in Eq. (5)

$$\sigma' = \sigma - p_p \quad (5)$$

where σ is total stress which can be calculated by the external load in the experiment. p_p is pore pressure. Then, we have

$$K_{eff} = K_{int0} \left(1 - \frac{(\ln(\sigma - p_p) - \ln \sigma'_0)(\lambda_0 - a s_h^b)}{\phi_0} \right)^\beta (1 - s_h)^N \quad (6)$$

The change in hydrate saturation during hydrate dissociation can be calculated using dissociation kinetic model. Definitely, it should be coupled with deformation, which has been shown in our previous paper[17,18]. Here, we use $s_h(\phi, p_p, T)$ to describe the dependence of hydrate saturation on porosity, pore pressure and

temperature. Therefore, Eq. (6) can be directly used to estimate the permeability change with pore pressure.

Table 2 Coefficients of the model obtained from the test data

λ_0	β	N
0.0269	1.4	2.024

The coefficients β , N and λ_0 in Table 2 are obtained by fitting the data in Fig.3, Fig. 4 and Fig. 2 using Eq. (1), Eq. (2) and Eq. (3) respectively. R^2 value for these three fitting curves is equal to 0.9369, 0.9820 and 0.9728 respectively. The variation of the effective permeability can be described by substituting all the coefficients into the Eq. (6), and can be quantified with the analysis of hydrate dissociation kinetics. Assuming that (1) the external load remains constant of 13.1MPa; (2) pore pressure decreases from 13MPa to 4MPa over one day; (3) temperature is maintaining during hydrate dissociation meaning that heat supply is sufficient; (4) initial hydrate saturation is equal to 0.5; (5) the coefficients corresponding to hydrate enhanced compressibility equals 0.003 and 2 respectively, the variation of effective permeability during hydrate dissociation by depressurization is shown in Fig. 5.

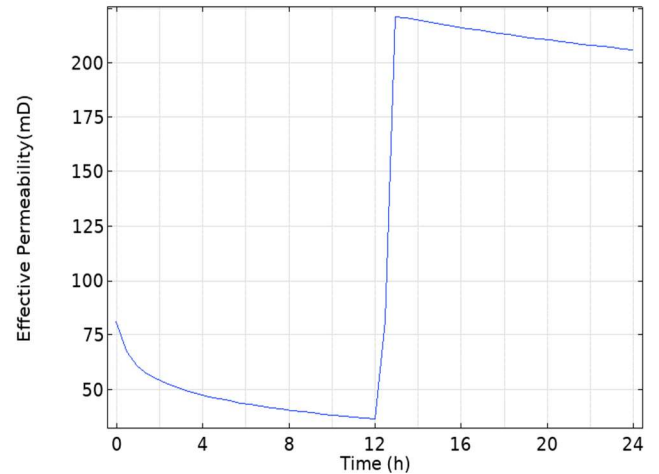


Fig.5 Change in effective permeability during depressurization

4. CONCLUSIONS

This paper proposes a method for estimating the effective permeability of hydrate-bearing sediments during hydrate production by depressurization. The variation is recognized as a combination of the effects of

compaction and hydrate dissociation. Both of them are investigated by a series of seepage experiments.

The experiments show that for the quartz sand, the intrinsic permeability decreases with soil compaction and the increase in hydrate saturation. Masuda's model and Ren's model can be used to fit the experimental data well and estimate the transient change in permeability during hydrate dissociation by depressurization. Combining with the relationship between porosity and effective stress and hydrate dissociation kinetics model, the variation in effective permeability can be described by changing pore pressure directly.

ACKNOWLEDGMENT

This study was supported by the National Natural Science Foundation of China (Grant Nos. 51876029 and 51890911), and the National Key Research and Development Program of China (Grant Nos. 2017YFC0307305, 2016YFC0304001, and 2017YFC0307705).

REFERENCE

[1] Sloan ED. Fundamental principles and applications of natural gas hydrates. *Nature* 2003;426:353-9. doi:10.1038/nature02135.

[2] Milkov AV. Global estimates of hydrate-bound gas in marine sediments: how much is really out there? *Earth-Science Reviews* 2004;66:183-97. doi:10.1016/j.earscirev.2003.11.002.

[3] Zhang L, Yang L, Wang J, Zhao J, Dong H, Yang M, Liu Y, Song Y. Enhanced CH₄ recovery and CO₂ storage via thermal stimulation in the CH₄/CO₂ replacement of methane hydrate. *Chemical Engineering Journal* 2017;308:40-49. doi:10.1016/j.cej.2016.09.047.

[4] Dong H, Zhang L, Ling Z, Zhao J, Song Y. The Controlling Factors and Ion Exclusion Mechanism of Hydrate-Based Pollutant Removal 2019;7(8):7932-40. doi:10.1021/acssuschemeng.9b00651.

[5] Zhao J, Guo X, Sun M, Zhao Y, Yang L, Song Y. N₂O hydrate formation in porous media: A potential method to mitigate N₂O emissions 2019; 361: 12-20. doi:10.1016/j.cej.2018.12.051.

[6] Zhang L, Zhao J, Dong H, Zhao Y, Liu Y, Zhang Y, Song Y. Magnetic resonance imaging for in-situ observation of the effect of depressurizing range and rate on methane hydrate dissociation 2016; 144: 135-143. doi:10.1016/j.ces.2016.01.027.

[7] Jang J, Santamarina JC. Evolution of gas saturation and relative permeability during gas production from hydrate-bearing sediments: Gas invasion vs. gas nucleation. *Journal of Geophysical Research: Solid Earth* 2014;119:116-26. doi:10.1002/2013JB010480.

[8] Moridis G, Kowalsky M, & KP-SRE, 2007 undefined. Depressurization-induced gas production from class-1 hydrate deposits. *OnePetroOrg* n.d.

[9] Kossel E, Deusner C, Bigalke N, Haeckel M. The Dependence of Water Permeability in Quartz Sand on Gas Hydrate Saturation in the Pore Space. *Journal of Geophysical Research: Solid Earth* 2018;123:1235-51. doi:10.1002/2017JB014630.

[10] Chen B, Yang M, Zheng J, Wang D, Song Y. Measurement of water phase permeability in the methane hydrate dissociation process using a new method. *International Journal of Heat and Mass Transfer* 2018;118:1316-24. doi:10.1016/j.ijheatmasstransfer.2017.11.085.

[11] Dai S, Kim J, Xu Y, Waite WF, Jang J, Yoneda J, et al. Permeability anisotropy and relative permeability in sediments from the National Gas Hydrate Program Expedition 02, offshore India. *Marine and Petroleum Geology* 2018:0-1. doi:10.1016/j.marpetgeo.2018.08.016.

[12] Wu Z, Li Y, Sun X, Wu P, Zheng J. Experimental study on the effect of methane hydrate decomposition on gas phase permeability of clayey sediments. *Applied Energy* 2018;230:1304-10. doi:10.1016/j.apenergy.2018.09.053.

[13] Mahabadi N, Dai S, Seol Y, Jang J. Impact of hydrate saturation on water permeability in hydrate-bearing sediments. *Journal of Petroleum Science and Engineering* 2019;174:696-703. doi:10.1016/j.petrol.2018.11.084.

[14] Dai S, Seol Y. Water permeability in hydrate-bearing sediments: A pore-scale study. *Geophysical Research Letters* 2014;41:4176-84. doi:10.1002/2014GL060535.

[15] Ren XW, Santamarina JC. The hydraulic conductivity of sediments: A pore size perspective. *Engineering Geology* 2018;233:48-54. doi:10.1016/j.enggeo.2017.11.022.

[16] Masuda Y, Fujinaga Y, Naganawa S, Fujita K, Sato K, Hayashi Y. Modeling and experimental studies on dissociation of methane gas hydrates in Berea sandstone cores. vol. 7, 1999, p. 18-22.

[17] Sun X, Luo H, Luo T, Song Y, Li Y. Numerical study of gas production from marine hydrate formations considering soil compression and hydrate dissociation due to depressurization. *Marine and Petroleum Geology* 2019;102:759-74.

[18] Sun X, Wang L, Luo H, Song Y, Li Y. Numerical modeling for the mechanical behavior of marine gas hydrate-bearing sediments during hydrate production by depressurization. *Journal of Petroleum Science and Engineering* 2019.